Phonon-Mediated Nonequilibrium Interaction between Nanoscale Devices

G. J. Schinner,[1] H. P. Tranitz,[2] W. Wegscheider,[2] J. P. Kotthaus,[1] and S. Ludwig[1]

[1]*Center for NanoScience and Fakultät für Physik, Ludwig-Maximilians-Universität, Geschwister-Scholl-Platz 1, 80539 München, Germany*

[2]*Institut für Experimentelle und Angewandte Physik, Universität Regensburg, 93040 Regensburg, Germany*

(Received 22 January 2009; published 5 May 2009)

Interactions between mesoscopic devices induced by interface acoustic phonons propagating in the plane of a two-dimensional electron system (2DES) are investigated by phonon spectroscopy. In our experiments, ballistic electrons injected from a biased quantum point contact emit phonons and a portion of them are reabsorbed exciting electrons in a nearby degenerate 2DES. We perform energy spectroscopy on these excited electrons employing a tunable electrostatic barrier in an electrically separate and unbiased detector circuit. The transferred energy is found to be bounded by a maximum value corresponding to Fermi-level electrons excited and backscattered by absorbing interface phonons. Our results imply that phonon-mediated interaction plays an important role for the decoherence of solid-state-based quantum circuits.

DOI: 10.1103/PhysRevLett.102.186801 PACS numbers: 73.63.−b, 03.67.−a, 68.65.−k, 73.23.−b

Nanoscale electronic circuits dominate present information technologies. Based on their coherent dynamics they are also considered as candidates for future quantum information processing [1,2]. Therefore, it is important to understand and control decoherence-inducing processes, such as the nonequilibrium backaction of a biased quantum point contact (QPC), widely used as single electron detector. However, the details of the relevant backaction mechanisms are not yet understood and a matter of ongoing investigations [3–7].

Phonon-induced currents in a two-dimensional electron system (2DES) have been evidenced in thermopower experiments [8,9] and also directly imaged with ballistically injected phonons [10]. In our experiments we employ a spectrometer, conceptually similar to a so-called lateral tunneling hot-electron amplifier [11], to analyze the energy of excited electrons in a 2DES and to study energy transfer mechanisms between mesoscopic circuits.

The inset of Fig. 1(a) sketches the calibration procedure of the energetic height E_{B_a} of an analyzer barrier B_a to be employed for quantitative energy spectroscopy. Hot electrons, injected across a barrier B_i into a degenerate Fermi (F)-sea of cold electrons, move ballistically with an excess kinetic energy of $E_{kin} - E_F \leq |eV_{SD}|$ towards B_a. As long as $E_{B_a} < E_{kin}$ some of these electrons pass B_a resulting in an analyzer (a) current I_a, while I_a vanishes for $E_{B_a} > E_{kin}$. The onset of $I_a(V_{SD})$ at $E_{B_a} = E_F + |eV_{SD}|$ serves as calibration of the barrier height E_{B_a}. The result of such a measurement is plotted in Fig. 1(a) displaying I_a (gray scale and contour lines) as a function of the gate voltage V_{B_a} and the bias V_{SD}. The ballistic motion of the electrons insures a straight line of current onset (purple), converting the gate voltage V_{B_a} [bottom scale of Fig. 1(a)] to the barrier height E_{B_a} (top scale). For $E_{B_a} < E_F$ a calibration is obtained by utilizing quantization of the electronic density of states into Landau levels with known energies in a perpendicular magnetic field [12–14].

A scanning electron micrograph of our spectrometer is pictured in Fig. 1(b). It is a mesoscopic Hall bar shaped by wet etching from a GaAs/AlGaAs heterostructure. The Hall bar contains 90 nm below the surface a 2DES with a Fermi energy of $E_F \simeq 14$ meV and an electron elastic mean free path of $l_m \simeq 14$ μm. Three 300 nm wide top gates [light gray in Fig. 1(b)] are designed to cross the entire Hall bar. By applying negative voltages to these gates, tunable potential barriers (B1, B2, and B3), completely suppressing tunneling, can be realized [15]. In addition, at each end of the Hall bar a QPC can be electrostatically defined by a pair of top gates. All experiments are performed in a dilution refrigerator at a base temperature of $T_{bath} = 20$ mK, applying a dc voltage to one of the Ohmic contacts of the otherwise grounded Hall bar. Currents are detected using a low noise current voltage amplifier at room temperature.

To spectroscopically study the energy transfer mechanisms between two adjacent mesoscopic devices we bias one of the barriers (B1) with a large negative voltage. As a result B1 is opaque for electrons and electrically separates the driven injector circuit from an unbiased detector circuit, as sketched in Fig. 2(a). In the emitter circuit hot ballistic electrons injected across a QPC (QPC1) are reflected between barrier B1 and QPC1. The hot electrons relax their excess energy in part by scattering with cold electrons or by emitting phonons. The injected excess charge drains to a grounded side contact. In the detector circuit barrier B2 is left open for electrons ($E_{B2} \ll E_F$) and B3 is used as analyzer barrier.

Although the detector circuit is unbiased we observe a current I_3 across the analyzer barrier B3. Hence, energy is transmitted across B1 while electrons are always reflected.

 © 2009 The American Physical Society

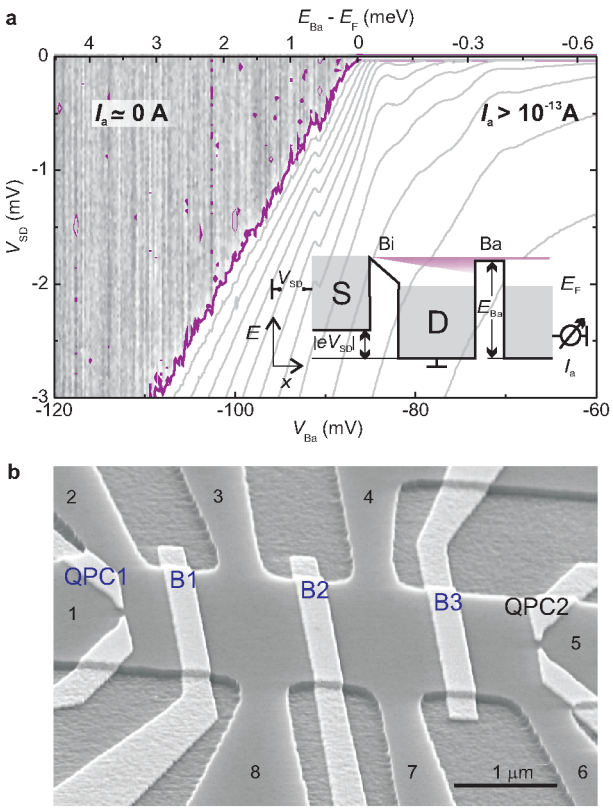

FIG. 1 (color online). (a) *Barrier calibration:* Inset: calibration setup (for details see main text). Main figure: Current I_a (gray scale for $I_a < 100$ fA, contour lines of constant current spaced by a factor of 3.3 for $I_a > 100$ fA) as a function of V_{SD} and the gate voltage V_{B_a}. The current onset ($I_a \simeq 100$ fA), highlighted in purple, serves as calibration. The resulting energy scale is displayed on the top axis. (b) Sample geometry: A Hall-bar (dark gray) with eight Ohmic contacts $(1, 2, \ldots, 8)$ is shaped from a GaAs/AlGaAs-heterostructure using electron-beam lithography (scanning electron micrograph). The Hall-bar is partly covered by metal gates (light gray) used to electrostatically define potential barriers (B1, B2, B3) and quantum point contacts (QPC1, QPC2).

In Fig. 2(a) the measured I_3 is displayed for a large bias regime -60 mV $\leq V_{SD} \leq 0$ and as a function of the excess barrier height $E_{B3} - E_F$. Strikingly, even at a large energy of injected electrons $|eV_{SD}| = 60$ meV, the analyzer current vanishes whenever the analyzer barrier height exceeds $E_{B3} \simeq E_F + 1.3$ meV. This observation implies that the maximum energy that can be transferred to equilibrium electrons in the detector circuit is $\Delta E^{max} \equiv E_{kin} - E_F \simeq 1.3$ meV. To further illustrate this exceptional behavior several $I_3 - E_{B3}$ traces at constant V_{SD} [indicated by horizontal lines in Fig. 2(a)] are plotted in Fig. 2(b). The larger the injection energy $|eV_{SD}|$ the sharper is the current onset at $E_{B3} - E_F \simeq \Delta E^{max}$.

At low temperatures energy exchange between mesoscopic circuits is usually attributed to Coulomb interaction as indeed observed in Coulomb-drag experiments [16–19]. Here, in our experiments, the upper bound ΔE^{max} of energy

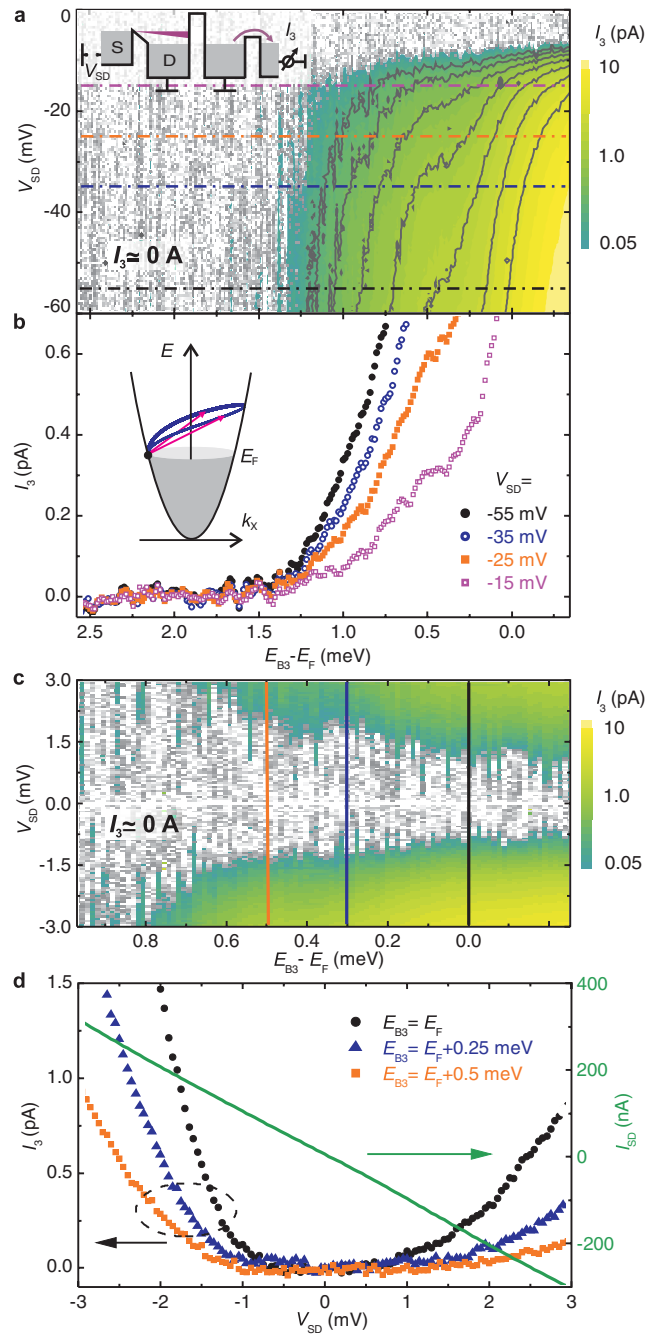

FIG. 2 (color online). *Phonon-driven current:* (a) Analyzer current $I_3 = I_a$ (gray scale, color for $I_3 \geq 50$ fA) across B3 (as analyzer barrier B_a) as a function of its energetic height $E_{B3} - E_F$ in the bias range $0 \geq V_{SD} \geq -60$ mV applied across QPC1 (as emitter). Barrier B1 is opaque for electrons and separates emitter and detector as sketched in the inset. B2 is left open ($E_{B2} \ll E_F$). Contour lines of constant current are spaced by a factor of 1.7. (b) $I_3 - E_{B3}$ traces along the horizontal lines in (a). The inset sketches relevant phonon absorption processes for an electron at the Fermi-level E_F. (c) Analyzer current I_3 in the bias range 3 mV $\geq V_{SD} \geq -3$ mV. Currents comparable to those at larger bias are achieved by lowering the injector barrier resistance. For the detailed configuration see main text. (d) I_3-V_{SD} traces along the vertical lines in (c). Also plotted is the injector current I_{SD} (right-hand side axis).

quanta transferred between emitter and detector reflects that the energy is mediated by interface acoustic phonons: Hot injected electrons can relax by emission of acoustic phonons [20]. In contrast to electrons, acoustic phonons can pass the electrostatic barrier (B1) between emitter and detector circuits. Energy and momentum conservation restrict the emission of interface acoustic phonons by electrons with momentum $\hbar k_e$ to momenta $k_{\rm ph} \lesssim 2\hbar k_e$, corresponding to backscattered electrons in the 2DES. With the same consideration only interface acoustic phonons with $k_{\rm ph} \lesssim 2\hbar k_{\rm F}$ can be absorbed by equilibrium electrons in the detector. This situation is indicated in the inset of Fig. 2(b), picturing the parabolic electron dispersion relation within the 2DES. The blue line indicates all possible states the electron (black circle), originally at the Fermi energy, can be scattered into by absorption of an interface acoustic phonon. Thus scattered electrons drive the analyzer current in the detector circuit. With the upper bound $\Delta E^{\rm max}$ measured and the known Fermi momentum $\hbar k_{\rm F}$ in the 2DES we obtain with $\Delta E^{\rm max} \simeq E_{\rm ph}(2k_{\rm F}) = 2\hbar k_{\rm F} v_{\rm s}$ a sound (s) velocity of $v_{\rm s} \simeq 6$ km/s, in good agreement with literature values of $v \simeq 5.3$ km/s for longitudinal acoustic phonons propagating in bulk-GaAs in the [110] direction [21], the orientation of our Hall bar. Our experiments show conclusively that the analyzer current is caused by both energy and momentum imbalance of nonequilibrium electrons excited by absorption of interface acoustic phonons in the unbiased detector circuit.

With increasing $V_{\rm SD}$ high energy electrons can emit phonons with momenta exceeding by far $2\hbar k_{\rm F}$. However, momentum conservation requires that these phonons have a large momentum component perpendicular to the 2DES [10]. At low temperatures they propagate ballistically through the bulk crystal with a mean-free path beyond the crystal dimensions [10,22]. As a consequence, only interface phonons are likely to be reabsorbed in the 2DES of the detector circuit and contribute to the analyzer current I_3. Correspondingly, the measured I_3 is typically 5 orders of magnitude smaller than the injector current $I_{\rm SD}$.

To avoid excessive power dissipation at large $|V_{\rm SD}|$, QPC1 is tuned to be highly resistive. For $|V_{\rm SD}| \lesssim 8$ mV QPC1 is even completely closed, $I_{\rm SD}$ vanishes, and therefore also I_3 [horizontal onset in Fig. 2(a)]. In order to explore electron-phonon scattering at small energies we instead tune barrier B2 to be opaque for electrons and employ B1 as an injector adjusted to a smaller resistance. The corresponding measurement is shown in Fig. 2(c), displaying the analyzer current I_3 as a function of $E_{\rm B3} - E_{\rm F}$ in the bias range -3 mV $\leq V_{\rm SD} \leq 3$ mV. Figure 2(d) plots $I_3 - V_{\rm SD}$ traces for constant $E_{\rm B3}$ [along the vertical lines in Fig. 2(c)]. Also shown is the measured injector current $I_{\rm SD}$ versus $V_{\rm SD}$ (right-hand side axis). It forms a straight line reflecting that B1 acts as a constant resistance. Nevertheless, I_3 still vanishes for $|V_{\rm SD}| \lesssim 0.8$ mV, independent of the analyzer barrier height $E_{\rm B3}$ [Figs. 2(c) and 2(d)]. Such a low-energy onset suggests that the interaction mechanism between emitter and detector strongly depends on energy. Note that energy transfer mediated by interface acoustic phonons is expected to strongly increase as their momenta approach $2\hbar k_{\rm F}$ [see inset in Fig. 2(b)] [20,23]. Similar onsets have been observed in recent experiments on interacting mesoscopic circuits [4,24]. No such onset behavior has been reported in experiments where the energy transfer between mesoscopic systems is mediated by potential fluctuations caused by moving charges [3,5].

In Fig. 2(c) we find $I_3 > 0$ independent of the sign of $V_{\rm SD}$. Clearly, the detector circuit acts as a unidirectional current source, driven by phonons originating in the emitter. In the electrically separate detector electrons absorb such interface phonons predominantly close to the emitter. Then the excited electrons move in the direction of the transferred momentum towards barrier B3 where they can contribute to the analyzer current I_3. The latter is considerably smaller for $V_{\rm SD} > 0$ compared to the case of $V_{\rm SD} < 0$. We relate this to the initial momentum of the hot electrons in the emitter which is for $V_{\rm SD} > 0$ directed away from the detector. In this case and in contrast to $V_{\rm SD} < 0$ an additional scattering process is needed to reverse the momentum towards the detector.

Compared to elastic scattering of ballistic electrons at the Fermi surface [25] nonequilibrium interactions at higher energies remain a challenging subject. Hot electrons can relax their excess energy either via electron-electron scattering [26–29], via electromagnetic fields generated by charge fluctuations [3,5,6], or via the emission of phonons [20,30,31]. Inelastic electron-phonon scattering in the 2DES for electrons with an excess energy of $\Delta E \simeq 1$ meV results in a mean-free path of $l_{e\text{-ph}} \sim 100$ μm [20,28,32] considerably longer than the electron-electron scattering length of $l_{e\text{-}e} \sim 8$ μm [33]. Both length scales are longer than the elastic mean-free path of electrons, limited to $l_{\rm m} \sim 1$ μm by the geometric boundaries of the device. In Fig. 3 we investigate the length scale $l_{\text{ph-}e}$ of the reabsorption of interface acoustic phonons within the 2DES. We compare two different experimental situations as sketched in the inset of Fig. 3. Configuration 1 is essentially identical to the one established in the experiment of Figs. 2(a) and 2(b) and displays the phonon-driven current as a function of $V_{\rm SD}$ with the analyzer barrier adjusted to $E_{\rm B3} \simeq E_{\rm F}$. In configuration 2 an additional barrier (B2) is raised well above the Fermi level ($E_{\rm B2} \gg E_{\rm F}$). Now the resulting phonon-driven current is about a factor of 10 smaller compared to configuration 1 but exhibits almost the same dependence on $V_{\rm SD}$. This finding implies that most phonons passing B1 are reabsorbed by the 2DES before reaching barrier B2 and thus cannot contribute to the phonon-driven current. As the distance between barriers B1 and B2 is 1 μm we consider this as an upper limit for the interface phonon mean-free path $l_{\text{ph-}e}$. The corresponding transition rates of $\sim(200\ {\rm ps})^{-1}$ agree roughly with theoretical estimates [20,32] and $l_{\text{ph-}e}/l_{e\text{-ph}}$ is

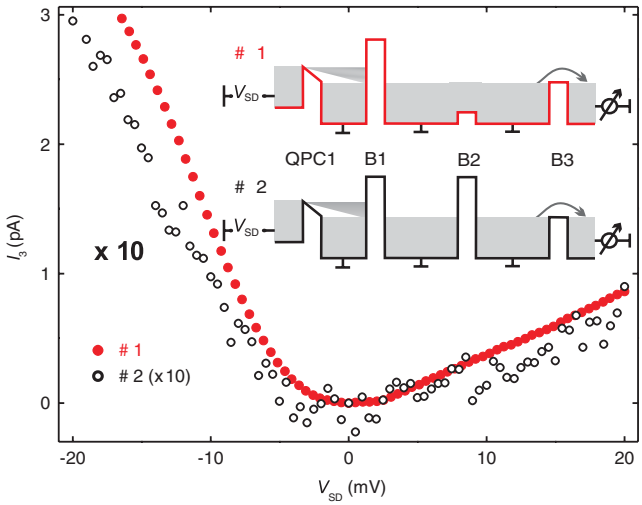

FIG. 3 (color online). *Mean-free path of interface acoustic phonons:* Analyzer current I_3 as a function of the emitter bias V_{SD} for the two experimental setups sketched in the inset. In setup 1 B2 is left open [as for Fig. 2(a)] while in setup 2 both barriers B1 and B2 are opaque for electrons. The analyzer barrier is tuned to $E_{B3} \simeq E_F$. In setup 2 I_3 is reduced by about a factor of 10. Hence, the distance between B1 and B2 of about 1 μm roughly corresponds to the phonon mean-free path.

of the order of the ratio of sound and Fermi velocity, as expected.

In conclusion, our experiments on interacting nonequilibrium mesoscopic circuits underline the importance of energy transfer mediated via interface acoustic phonons and generated by ballistically moving electrons driven out of equilibrium. In particular, they demonstrate conclusively that this energy transfer between a nonequilibrium nanoscale circuit, serving as emitter, and an adjacent detector circuit is bounded by the energy of interface acoustic phonons with momentum $2\hbar k_F$. This is the maximum momentum that can be transferred to equilibrium electrons under conservation of momentum and energy. Since such phonon-mediated interactions reduce the coherence times of quantum states in confined electron systems their study and understanding is important for the realization of semiconductor-based coherent quantum devices. Beyond we establish a method to spectroscopy interface acoustic phonons in a new regime up to momenta of $2\hbar k_F$.

We thank A. O. Govorov, W. Dietsche, M. Heiblum, V. S. Khrapai, and K. F. Renk for stimulating discussions and D. Harbusch, D. Taubert, M. Kroner as well as S. Seidl for helpful comments. Financial support by the German Science Foundation via SFB 631, the Germany Israel program DIP and the German Excellence Initiative via the "Nanosystems Initiative Munich (NIM)" is gratefully acknowledged.

[1] J. R. Petta *et al.*, Science **309**, 2180 (2005).
[2] F. H. L. Koppens *et al.*, Nature (London) **442**, 766 (2006).
[3] E. Onac *et al.*, Phys. Rev. Lett. **96**, 176601 (2006).
[4] V. S. Khrapai, S. Ludwig, J. P. Kotthaus, H. P. Tranitz, and W. Wegscheider, Phys. Rev. Lett. **97**, 176803 (2006).
[5] S. Gustavsson *et al.*, Phys. Rev. Lett. **99**, 206804 (2007).
[6] S. Gustavsson, I. Shorubalko, R. Leturcq, T. Ihn, K. Ensslin, and S. Schön, Phys. Rev. B **78**, 035324 (2008).
[7] D. Taubert, M. Pioro-Ladrière, D. Schröer, D. Harbusch, A. S. Sachrajda, and S. Ludwig, Phys. Rev. Lett. **100**, 176805 (2008).
[8] R. Fletcher, M. D'Iorio, A. S. Sachrajda, R. Stoner, C. T. Foxon, and J. J. Harris, Phys. Rev. B **37**, 3137 (1988).
[9] C. Ruf, H. Obloh, B. Junge, E. Gmelin, K. Ploog, and G. Weimann, Phys. Rev. B **37**, 6377 (1988).
[10] H. Karl, W. Dietsche, A. Fischer, and K. Ploog, Phys. Rev. Lett. **61**, 2360 (1988).
[11] A. Palevski, C. P. Umbach, and M. Heiblum, Appl. Phys. Lett. **55**, 1421 (1989).
[12] R. J. Haug, A. H. MacDonald, P. Streda, and K. von Klitzing, Phys. Rev. Lett. **61**, 2797 (1988).
[13] S. Komiyama, H. Hirai, S. Sasa, and S. Hiyamizu, Phys. Rev. B **40**, 12566 (1989).
[14] An additional calibration point is obtained by measuring the linear response current across B_a for $E_{B_a} = E_F$. All three calibration methods are consistent.
[15] Barriers $B1$, $B2$, $B3$ are calibrated with likewise results.
[16] T. J. Gramila, J. P. Eisenstein, A. H. MacDonald, L. N. Pfeiffer, and K. W. West, Phys. Rev. Lett. **66**, 1216 (1991).
[17] U. Sivan, P. M. Solomon, and H. Shtrikman, Phys. Rev. Lett. **68**, 1196 (1992).
[18] M. P. Lilly, J. P. Eisenstein, L. N. Pfeiffer, and K. W. West, Phys. Rev. Lett. **80**, 1714 (1998).
[19] M. Yamamoto, M. Stopa, Y. Tokura, Y. Hirayama, and S. Tarucha, Science **313**, 204 (2006).
[20] B. K. Ridley, Rep. Prog. Phys. **54**, 169 (1991).
[21] J. S. Blakemore, Appl. Phys. **53**, R123 (1982).
[22] D. Lehmann and C. Jasiukiewicz, Turk. J. Phys. **23**, 583 (1999).
[23] The 2DES screens the piezoelectric coupling between electrons and interface phonons with small k vectors. This screening effect hinders the emission and absorption of low energy interface phonons and might very well contribute to the observed low-energy onset.
[24] V. S. Khrapai, S. Ludwig, J. P. Kotthaus, H. P. Tranitz, and W. Wegscheider, Phys. Rev. Lett. **99**, 096803 (2007).
[25] C. W. J. Beenakker and H. v. Houten, Solid State Phys. **44**, 1 (1991).
[26] I. I. Kaya and K. Eberl, Phys. Rev. Lett. **98**, 186801 (2007).
[27] A. O. Govorov and J. J. Heremans, Phys. Rev. Lett. **92**, 026803 (2004).
[28] H. Predel *et al.*, Phys. Rev. B **62**, 2057 (2000).
[29] A. V. Chaplik, Sov. Phys. JETP **33**, 997 (1971).
[30] U. Sivan, M. Heiblum, and C. P. Umbach, Phys. Rev. Lett. **63**, 992 (1989).
[31] A. S. Dzurak *et al.*, Phys. Rev. B **45**, 6309 (1992).
[32] U. Bockelmann and G. Bastard, Phys. Rev. B **42**, 8947 (1990).
[33] G. F. Giuliani and J. J. Quinn, Phys. Rev. B **26**, 4421 (1982).